

## GENERAL INSTRUCTION

- **Authors:** Please check and confirm whether the name of the corresponding author is correct as set.
- **Authors:** Carefully check the page proofs (and coordinate with all authors); additional changes or updates WILL NOT be accepted after the article is published online/print in its final form. Please check author names and affiliations, funding, as well as the overall article for any errors prior to sending in your author proof corrections.
- **Authors:** We cannot accept new source files as corrections for your article. If possible, please annotate the PDF proof we have sent you with your corrections and upload it via the Author Gateway. Alternatively, you may send us your corrections in list format. You may also upload revised graphics via the Author Gateway.

### Queries

- Q1. Author: Please confirm or add details for any funding or financial support for the research of this article.
- Q2. Author: Please provide the expansions for the acronyms LP and DC-OPF at the instances when they are first mentioned in the text.
- Q3. Author: Please provide complete bibliographic details for Refs. [25] and [30].
- Q4. Author: Please provide update for Refs. [26] and [28], if already published.
- Q5. Author: Please provide the subject in which the authors Juan Miguel Morales and Salvador Pineda received the Ingeniero Industrial degree.

# Unifying Chance-Constrained and Robust Optimal Power Flow for Resilient Network Operations

Álvaro Porras, Line Roald <sup>1b</sup>, *Member, IEEE*, Juan Miguel Morales <sup>1b</sup>, *Senior Member, IEEE*, and Salvador Pineda <sup>1b</sup>, *Senior Member, IEEE*

**Abstract**—Uncertainty in renewable energy generation has the potential to adversely impact the operation of electric networks. Numerous approaches to manage this impact have been proposed, ranging from stochastic and chance-constrained programming to robust optimization. However, these approaches either tend to be conservative or leave the system vulnerable to low-probability, high-impact uncertainty realizations. To address this issue, we propose a new formulation for stochastic optimal power flow that explicitly distinguishes between “normal operation,” in which automatic generation control (AGC) is sufficient to guarantee system security, and “adverse operation,” in which the system operator is required to take additional actions, e.g., manual reserve deployment. The new formulation has been compared with the classical ones in a case study on the IEEE-118 and IEEE-300 bus systems. We observe that our consideration of extreme scenarios enables solutions that are more secure than typical chance-constrained formulations, yet less costly than solutions that guarantee robust feasibility with only AGC.

**Index Terms**—Automatic generation control (AGC), chance constraints, manual adjustment, optimal power flow (OPF), wind power.

## NOMENCLATURE

The main notation used throughout the text is stated below for quick reference.

Manuscript received 17 January 2024; accepted 12 May 2024. Date of publication; date of current version. This work was supported in part by the Spanish Ministry of Science and Innovation through project PID2020-115460GB-I00 under Grant AEI/10.13039/501100011033 and in part by the European Research Council (ERC) through the European Union’s Horizon 2020 research and innovation programme under Grant 755705. The work of Álvaro Porras was supported by the Spanish Ministry of Science, Innovation and Universities through the university teacher training program with fellowship number FPU19/03053. The work of Line Roald was supported by the Department of Energy, Office of Science, Office of Advanced Scientific Computing Research, Applied Mathematics program under Grant DE-AC02-06CH11347. Recommended by Associate Editor P. Barooah. (*Corresponding author: Juan Miguel Morales.*)

Álvaro Porras, Juan Miguel Morales, and Salvador Pineda are with the OASYS Research Group, University of Malaga, 29010 Malaga, Spain (e-mail: alvaroporras19@gmail.com; juanmi82mg@gmail.com; spineda@uma.es).

Line Roald is with the Department of Electrical and Computer Engineering, University of Wisconsin Madison, Madison, WI 53707 USA (e-mail: roald@wisc.edu).

Digital Object Identifier 10.1109/TCNS.2024.3432188

<i>A. Sets</i>		32
$\mathcal{G}$	Set of generating units, indexed by $g$ .	33
$\mathcal{L}$	Set of transmission lines, indexed by $l$ .	34
$\mathcal{N}$	Set of nodes, indexed by $n$ .	35
<i>B. Parameters</i>		36
$c_g$	Linear operating cost of generating unit $g$ [€/MWh].	37
$c_g^d/c_g^u$	Downward/upward reserve capacity cost of generating unit $g$ [€/MW].	38
$c_g^-/c_g^+$	Downward/upward reserve cost of generating unit $g$ [€/MWh].	39
$B_{ln}$	Power transfer distribution factor (PTDF) of transmission line $l$ with respect to node $n$ .	40
$d_n$	Forecasted demand at node $n$ [MW].	41
$\bar{f}_l$	Maximum capacity of transmission line $l$ [MW].	42
$\frac{p_g}{\bar{p}_g}$	Minimum/maximum output of unit $g$ [MW].	43
$\frac{r_g^d}{\bar{r}_g^d}/\frac{r_g^u}{\bar{r}_g^u}$	Ability of generator $g$ to provide downward and upward reserves [MW].	44
$\tilde{w}_n$	Actual wind power production at node $n$ [MW].	45
$\hat{w}_n$	Forecasted wind power production at node $n$ [MW].	46
$\omega_n$	Error of the predicted wind power at node $n$ [MW].	47
<i>C. Variables</i>		48
$p_g$	Power output dispatch of unit $g$ [MW].	49
$r_g(\omega)$	Reserve deployed by unit $g$ [MW].	50
$r_g^-(\omega)/r_g^+(\omega)$	Downward/upward reserve deployed by unit $g$ [MW].	51
$r_g^d/r_g^u$	Downward/upward reserve capacity of unit $g$ [MW].	52
$\alpha_g(\omega)$	Manual adjustment of power output dispatch at unit $g$ [MW].	53
$\beta_g$	Participation factor of unit $g$ .	54

## I. INTRODUCTION

OPTIMIZATION under uncertainty is a challenging task, and even more so in network systems where uncertainty realizations in different parts of the network can collude to create unexpected difficulties in maintaining balanced network conditions and managing flow constraints. In many systems, it

is possible to distinguish between *normal operations*, where the system is operating as desired and (minor) disturbances can be managed using simple, automatic controls, and *adverse operations*, where system security is challenged and additional control actions may be necessary to “save” the system from significant impacts. It is typically desirable to limit the probability that the system enters into an adverse operating condition, i.e., to ensure that the normal operational controls are sufficient to guarantee constraint satisfaction with a high probability. However, it is also important to ensure that there exist effective controls to limit system impacts and recover feasible operations if we enter into an adverse operating condition. In this article, we address this problem by exploring a problem formulation that combines features of chance-constrained and robust optimization, and is related to the idea of chance-constrained programming with recovery proposed in [1]. To make our problem formulation concrete, we consider the problem of operating a power grid under uncertainty. However, similar problems of managing the probability of adverse operations and ensuring feasibility recovery in all scenarios could be applied to a range of other networks, including, e.g., supply chain networks, emergency response networks, and others.

#### 94 A. Electric Grid Operation Under Uncertainty

95 The optimal power flow (OPF) is a classical tool widely used  
96 for day-ahead and real-time power system operations, electricity  
97 markets, long-term planning, and many other applications [2].  
98 In its deterministic version, the OPF problem seeks to determine  
99 the least-costly dispatch of thermal generating units to satisfy the  
100 system’s demand, while complying with the technical limits of  
101 production and transmission network equipment [3]. However,  
102 the increasing integration of renewable energy sources into  
103 power systems leads to increased variability and uncertainty  
104 in both the power generation and associated power flows. Un-  
105 derstanding and quantifying the impact of this uncertainty on  
106 decision-making problems, such as the OPF, is crucial to ensure  
107 the secure operation of power systems [4].

108 Given this context, a large and growing body of work has  
109 addressed the stochastic version of the optimal power flow  
110 (SOPF) problem [5]. The SOPF aims to minimize expected  
111 operational cost and avoid constraint violations while consid-  
112 ering the uncertainty in its random parameters. Existing works  
113 deal with uncertainty in SOPF using different approaches, such  
114 as multistage stochastic programming [6]; robust or worst-case  
115 optimization [7], [8], [9]; or chance-constraints [10], [11], [12],  
116 [13], [14], [15]. The major challenge is to design a model that  
117 captures the risk of constraint violations and accurately reflects  
118 the operation of power systems, while maintaining computa-  
119 tional tractability.

#### 120 B. Activation of Generation Reserves

121 When modeling the impact of uncertain generation on short-  
122 term operations (i.e., day ahead until real time), it is common  
123 to assume that forecast errors and renewable energy variability  
124 will be balanced by the deployment of generation reserves, and in  
125 particular, by systems such as the *automatic generation control*  
126 (AGC) [16]. A benefit of modeling system balancing through

AGC is that it is naturally represented as an affine control  
policy, which also simplifies the solution of the optimization  
problem. However, the common AGC models implemented in  
the literature typically assume that all generators contribute  
reserve power according to the affine policy, even for large  
uncertainty deviations. In reality, generator output will saturate  
(or stop increasing/decreasing as the deviation grows larger)  
when they hit their lower or upper generation limit. Furthermore,  
operators generally take additional actions to manage both bal-  
ancing and congestion in situations with very large deviations.  
For example, the *North American Reliability Corporation* [17]  
standard for regulating the use of AGC, BAL-005, states that if  
the AGC becomes inoperative or may impair the reliability of the  
interconnection, the system operator must use manual controls  
to adjust generation in order to guarantee balance.

142 While a limited number of studies have shown that modeling  
143 generation saturation [18] or accounting for manual reserve  
144 activation during large deviations [19] leads to better operating  
145 conditions, these models are often computationally expensive.  
146 Thus, a more common approach is to apply the affine control  
147 policy, but explicitly disregard constraint satisfaction in a frac-  
148 tion of the most severe operating conditions. This is typically  
149 done by introducing chance constraints that allow violations  
150 in a (typically small) percentage of scenarios [10], [11], [12],  
151 [13], [14], [15], or by solving robust optimization formulations  
152 where the uncertainty set has been designed to contain a certain  
153 probability mass [20].

154 Unfortunately, by failing to model the impact of the worst  
155 scenarios (those for which the constraint satisfaction is dis-  
156 carded), a chance-constrained formulation may leave the system  
157 vulnerable to large disruptions that include generator and line  
158 outages, or load shed. As discussed in [12], there could be  
159 instances where the combination of generators and renewable  
160 outputs collude to produce power flows that significantly exceed  
161 the nominal line ratings, even in the absence of a large total power  
162 deviation. When the maximum rating of a line is exceeded, this  
163 line becomes more likely to trip, leaving the network vulnerable  
164 to cascading failures and associated load shed.

#### 165 C. Contributions

166 To address this issue, in this work, we propose a new SOPF  
167 formulation that distinguishes between two different operating  
168 regimes, namely, *normal operation* and *adverse operation*. In  
169 the SOPF context, *normal operation* refers to a situation, in  
170 which AGC is sufficient to maintain the system balance, while  
171 *adverse operation* refers to a situation, in which the system  
172 operator may need to implement additional actions, such as  
173 manual adjustments, to preserve system security.

174 Unlike the standard *joint chance-constrained* OPF (JCC-  
175 OPF), which limits the joint probability of violation of technical  
176 constraints, our formulation uses a joint chance-constraint to  
177 control the probability of utilizing different reserve actions.  
178 Thus, we can impose that AGC alone is to be sufficient with  
179 a high probability, while additional corrective actions are only  
180 to be implemented for the most adverse scenarios. In doing so,  
181 we reduce the need for frequent manual intervention by oper-  
182 ators (computational expensive), while also guaranteeing that

183 additional resources are available to handle adverse operating  
184 conditions, e.g., by scheduling more reserve capacity for manual  
185 deployment.

186 To demonstrate the suitability of our proposed formulation,  
187 we conduct a computational experiment that compared it to two  
188 state-of-the-art approaches. The former is the standard JCC-  
189 OPF, whose drawback is to leave the power system vulnerable  
190 to severe events, e.g., by dispatching insufficient generation  
191 capacity or giving up on alleviating congestion. The second  
192 approach guarantees robust feasibility using AGC only, which  
193 results in conservative solutions with increased operating costs,  
194 for instance, due to inefficient and oversized generation capacity.  
195 Our novel formulation results in decisions that are more reliable  
196 than the former approach and more cost-efficient than the latter.

197 The main contributions of this article are as follows.

- 198 1) We propose a novel OPF formulation that accounts for  
199 both adverse and normal operations and their relation  
200 to the various reserve actions employed in actual power  
201 system operations, such as AGC and manual redispatch.
- 202 2) Our problem formulation combines aspects of chance-  
203 constrained and robust optimization. We use a joint chance  
204 constraint to restrict the probability of entering adverse oper-  
205 ating conditions, while enforcing that feasibility recovery  
206 is possible for all scenarios with the use of additional  
207 controls. Specifically, we limit the probability of manual  
208 adjustments occurring instead of limiting the probability  
209 of violation of technical constraints, and guarantee that  
210 the use of manual controls ensures that the system remains  
211 feasible in all scenarios. This is representative of a realistic  
212 setting where the AGC operates under ordinary system  
213 conditions and the manual adjustments, which are not  
214 automatic, are implemented under adverse scenarios only.
- 215 3) We show that our approach provides an opportunity to  
216 obtain solutions that are different than existing chance-  
217 constrained and robust optimization approaches. In partic-  
218 ular, our approach yields solutions that are more reliable  
219 than the conventional joint chance-constrained DC-OPF,  
220 yet less costly than those approaches that guarantee robust  
221 feasibility with AGC alone.

222 The rest of this article is organized as follows. Section II  
223 describes the proposed SOPF formulation, which is derived  
224 from two traditional approaches in the literature. Section III  
225 describes the reformulation and algorithm used to make our  
226 proposal tractable and computationally efficient. Section IV  
227 explains the methodology we use to benchmark our approach,  
228 while Section V discusses experimental results from a case  
229 study. Finally, Section VI concludes this article.

## 230 II. PROBLEM FORMULATION

231 We start this section by introducing a standard and well-  
232 known formulation of the *joint chance-constrained DC-OPF*  
233 *problem*. We use this formulation as a basis to construct and  
234 motivate our proposed stochastic OPF formulation, which is  
235 presented immediately after.

236 Before diving into the detailed mathematical formulations,  
237 we would like to highlight some distinguishing features between

our proposed formulation and common stochastic optimization  
238 approaches. While our proposed formulation contains a joint  
239 chance constraint and thus is a chance-constrained program,  
240 there are some significant differences to common joint chance-  
241 constrained optimization. In our formulation, the chance con-  
242 straint controls the probability of manual reserve activation, not  
243 the probability of constraint violation. In a more general setting,  
244 the chance constraint can be seen as managing the probability  
245 of switching from normal to adverse operations. Furthermore,  
246 our proposed problem formulation guarantees that all scenarios  
247 can be made feasible by leveraging the additional controls (in  
248 our case manual reserve activation), and thus provides robust  
249 constraint satisfaction across scenarios. As such, our proposed  
250 formulation combines features of chance-constrained and robust  
251 optimization.

252 For notational simplicity, as in [14], we assume that there is  
253 one dispatchable generator, one uncertain power source (e.g., a  
254 wind farm), and one power load per node  $n$ . The power dispatch  
255 of the generator, the power produced by the uncertain power  
256 source, and the power consumed by the power load are denoted  
257 by  $p_n$ ,  $\tilde{w}_n$ , and  $d_n$ , respectively. The power  $\tilde{w}_n$  generated by  
258 the uncertain power source at node  $n$  is modeled as a random  
259 variable, which we decompose as  $\tilde{w}_n = \hat{w}_n + \omega_n$ , with  $\hat{w}_n$  being  
260 the forecast value (assumed unbiased) and  $\omega_n$  the associated  
261 forecast error. The system-wide aggregate forecast error is given  
262 by  $\Omega = \sum_{n \in \mathcal{N}} \omega_n$ , and translates into a system-wide power  
263 imbalance, which is balanced by the dispatchable generators  
264 through the deployment of reserve. The reserve deployment  
265 follows an affine control policy, modeling the actions of the  
266 AGC. According to this policy, the reserve provided by the  
267 generator at node  $n$  is given by  $r_n(\omega) = -\beta_n \Omega$ , where  $\beta_n$  is  
268 the participation factor and  $\omega$  represents the vector of power  
269 forecast errors across all nodes. Furthermore, we distinguish  
270 between *upward* or *positive* reserve  $r_n^+(\omega)$  and *downward* or  
271 *negative* reserve  $r_n^-(\omega)$ , with  $r_n(\omega) = r_n^+(\omega) - r_n^-(\omega)$ .

272 With this notation in place, the *joint chance-constrained DC-*  
273 *OPF problem* can be formulated as follows: 274

$$275 \min_{\Xi} \sum_n c_n p_n + c_n^u r_n^u + c_n^d r_n^d$$

$$276 + \mathbb{E} [c_n^+ r_n^+(\omega) - c_n^- r_n^-(\omega)] \quad (1a)$$

$$277 \text{s.t. } \sum_n \beta_n = 1 \quad (1b)$$

$$278 \sum_n (p_n + \hat{w}_n - d_n) = 0 \quad (1c)$$

$$279 p_n + r_n^d \leq p_n \leq \bar{p}_n - r_n^u \quad \forall n \quad (1d)$$

$$280 0 \leq r_n^d \leq \bar{r}_n^d \quad \forall n \quad (1e)$$

$$281 0 \leq r_n^u \leq \bar{r}_n^u \quad \forall n \quad (1f)$$

$$282 r_n^+(\omega) - r_n^-(\omega) = -\Omega \beta_n \quad \forall n \quad (1g)$$

$$283 \mathbb{P} \left( \begin{array}{l} -r_n^d \leq -\Omega \beta_n \leq r_n^u \quad \forall n \\ -\bar{f}_l \leq \sum_n B_{ln} (p_n - \Omega \beta_n + \\ + \hat{w}_n + \omega_n - d_n) \leq \bar{f}_l \quad \forall l \end{array} \right) \geq 1 - \epsilon \quad (1h)$$



$$\beta_n, r_n^+(\omega), r_n^-(\omega) \geq 0 \quad \forall n \quad (1i)$$

where  $\Xi = (p_n, r_n^+(\omega), r_n^-(\omega), r_n^d, r_n^u, \beta_n)$  is the set of decision variables. We remark that  $r_n^d$  and  $r_n^u$  are the downward and upward reserve capacity provided by the dispatchable generator at node  $n$ , respectively. This reserve capacity is procured by the system operator before the forecast errors  $\omega$  are known.

The three terms of the objective function (1a) to be minimized correspond to the power dispatch cost, the cost of procuring reserve capacity, and the expected cost related to the actual deployment of that capacity, respectively. The power balance in the system is guaranteed for all possible realizations of  $\omega$  through (1b) and (1c). Note that by requiring  $\beta_n \geq 0$  in (1i), we enforce that all reserve deployment only acts to counter-balance forecast errors, rather than also allowing redispatch among generators to counter congestion. Constraints (1d) ensure that the power produced and the reserve capacity offered by dispatchable generators are within their minimum and maximum power output limits  $\underline{p}_n$  and  $\bar{p}_n$ . This condition is expressed by adjusting the generation limits for the dispatchable generation by the respective reserve capacities each generator provides. Constraints (1e) and (1f) set a limit on the maximum reserve capacity each generator is willing or able to provide. Equation (1g) models the affine control policy for reserve deployment (AGC) we discussed above. Equation (1h) constitutes the joint chance-constraint system by which the system operator states that the reserves deployed and the line flows must be within their bounds with a probability greater than or equal to  $1 - \epsilon$ . Accordingly, the parameter  $\epsilon$  is the maximum allowed probability of constraint violation set by the operator to reflect their risk preferences. Note that by implementing a joint chance constraint (as opposed to, e.g., multiple single chance constraints), we can interpret  $\epsilon$  as a metric for overall system security. In the literature on chance constrained OPF,  $\epsilon$  is often chosen to be in the range from 0% to 10%. In (1h),  $l$  is the index of transmission lines in the power network and  $\bar{f}_l$  stands for the capacity limit of line  $l$ . Note that the joint chance constraint limits the probability that the reserve activation exceeds the contracted reserve capacities, and thus ensures, in combination with (1d), that the generation limits will be satisfied with a high probability. Finally, (1i) imposes the positive character of decision variables  $\beta_n$  and random functions  $r_n^+(\omega)$  and  $r_n^-(\omega)$  for all  $n$ . Note that the probability in (1h) is computed over the probability space of  $\omega$  and that the equality (1g) and the inequality (1i) must hold for almost all  $\omega$ .

The popularity of the joint chance-constrained formulation (1) stems from its ability to guarantee overall system security by ensuring that all constraints will remain satisfied with a high probability, while at the same time reducing the expected system operating cost substantially compared with robust optimization by allowing the violation of reserve capacity constraints and/or line flow limits under a small  $\epsilon$ -percentage of realizations of  $\omega$ . These realizations, or scenarios, are thus the most detrimental to the system in terms of cost. Parameter  $\epsilon$  in (1) controls the level of risk aversion of the system operator (a lower  $\epsilon$  implies more risk averse). If  $\epsilon$  is set to 0, formulation (1) becomes *robustly feasible*, meaning that all the constraints and variable limits are to be satisfied with probability one.

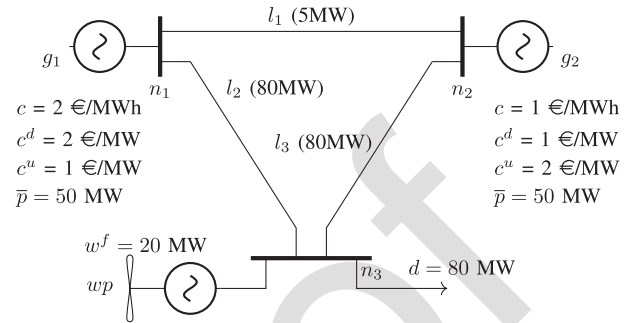


Fig. 1. Three-node illustrative example.

While chance-constrained OPF has gained widespread attention and is closely tied to existing criteria for reliability and reserve procurement, the critical nature of power systems practically forces operators to guarantee robust feasibility. Indeed, in those very few  $\omega$ -scenarios for which AGC is unable or too costly to ensure the system's integrity, the operators can still take over the affine control policy and *manually* set new operating points for some generators in the system, those needed to guarantee the satisfaction of the system's constraints ideally at the minimum cost. The fact that formulation (1) ignores the possible need for a manual control taking over AGC (albeit with a low occurrence) causes it to underestimate the operating cost when  $\epsilon > 0$  or overestimate it when robust feasibility is pursued ( $\epsilon = 0$ ). The ultimate result is that formulation (1) may produce uneconomical or suboptimal affine control policies.

To illustrate our point, we use an example based on the small power system depicted in Fig. 1. The system includes two thermal generating units with the linear production costs, reserve capacity costs, and maximum power limits indicated in the figure. For simplicity, the susceptances of all lines are assumed to be 1 per unit and the capacity of each line is also specified in the figure. A single demand of 80 MW is located at node  $n_3$ , where there is also a wind farm with a predicted output of 20 MW. We assume that the associated (random) forecast error can take on three different values only, namely, 20, 10, and  $-20$  MW, corresponding to three equally probable realizations or scenarios 1, 2, and 3 in that order. The costs of deploying upward and downward reserve, i.e.,  $c_n^+$  and  $c_n^-$ , are 1.2 and 0.8 times the generator's linear operating cost, respectively.

Results from problem (1) when  $\epsilon = 1/3$  and  $\epsilon = 0$  are shown in the first two rows of Table I. These results include the optimal power dispatch, participation factors, and procured reserve capacities, together with the optimal expected operating cost. Unsurprisingly, the results are quite sensitive to  $\epsilon$ . For example, when this is set to zero (to achieve robust feasibility), much more reserve capacity is to be procured than when we allow the system's constraints to be violated under one of the scenarios, in particular, scenario 3. Accordingly, the cost increases from €95 to €137.5, when  $\epsilon$  goes from 1/3 to 0. In contrast, if we take the solution delivered for  $\epsilon = 1/3$  and scenario 3 actually occurs, meaning that the wind power forecast error takes on the value  $-20$  MW, the AGC requires generator  $g_2$  to increase its production up to 65 MW, that is, above its maximum output

TABLE I  
 RESULTS—ILLUSTRATIVE EXAMPLE

Method	$p_1$	$p_2$	$\beta_1$	$\beta_2$	$r_1^u$	$r_2^u$	$r_1^d$	$r_2^d$	Cost (€)
model (1) ( $\epsilon = 1/3$ )	15	45	0	1	0	0	0	20	95
model (1) ( $\epsilon = 0$ )	12.5	47.5	0.625	0.375	12.5	7.5	12.5	7.5	137.5
model (3) ( $\epsilon = 1/3$ )	15	45	0	1	20	0	0	20	123

373 limit, while exceeding the maximum capacity of line  $l_1$  too.  
 374 But what is more important from a practical point of view is  
 375 that, under such a scenario, the solution to problem (1) when  
 376  $\epsilon = 1/3$  does *not* allow for any *manual redispatch* that can  
 377 restore system feasibility immediately after, because no upward  
 378 reserve capacity has been procured beforehand. Consequently,  
 379 formulation (1) may be too risky or too costly.

380 To address this issue, we propose a novel joint chance-  
 381 constrained formulation of the DC-OPF problem that does ac-  
 382 count for the possibility of resorting to a manual redispatch in  
 383 this  $\epsilon$ -percentage of events in which the implementation of AGC  
 384 is too expensive or even infeasible. Our approach involves the use  
 385 of manual adjustments to balance and ensure reliability under  
 386 extreme conditions, while model (1) with  $\epsilon = 0$  only employs  
 387 AGC and model (1) with  $\epsilon > 0$  does not consider any corrective  
 388 measures for adverse scenarios. To obtain our formulation, we  
 389 replace the set of constraints (1g) and (1h) in (1) with the  
 390 following ones:

$$\sum_n \alpha_n(\omega) = 0 \quad (2a)$$

$$r_n^+(\omega) - r_n^-(\omega) = -\Omega\beta_n + \alpha_n(\omega) \quad \forall n \quad (2b)$$

$$-r_n^d \leq -\Omega\beta_n + \alpha_n(\omega) \leq r_n^u \quad \forall n \quad (2c)$$

$$-\bar{f}_l \leq \sum_n B_{ln}(p_n - \Omega\beta_n + \alpha_n(\omega) + \hat{w}_n + \omega_n - d_n) \leq \bar{f}_l \quad \forall l \quad (2d)$$

$$\mathbb{P}(\alpha_n(\omega) = 0 \quad \forall n) \geq 1 - \epsilon \quad (2e)$$

391 where  $\alpha_n(\omega)$  is a random variable that represents the manual  
 392 adjustment of the power output of the generator located at  
 393 node  $n$ .

394 Equation (2a) is required for the implemented power adjust-  
 395 ments to preserve the power balance. Equation (2b) is analogous  
 396 to (1g), but including the manual adjustment requested by the  
 397 system operator. Inequalities (2c) and (2d) enforce that the use  
 398 of AGC in combination with manual redispatch guarantees that  
 399 the system's constraints are satisfied under any realization of  
 400  $\omega$ . Finally, in our proposal, chance-constrained programming is  
 401 employed for a different purpose than that in (1). Specifically, the  
 402 chance-constraint (2e) seeks to characterize the use of manual  
 403 control as an *occasional* recourse action, thus ensuring that  
 404 AGC is the standard control policy. Again, constraints (2a)–(2d)  
 405 are to be satisfied for almost all  $\omega$ .

406 Our proposal can thus be formulated as follows:

$$\begin{aligned} \min_{\Xi} \quad & \sum_n c_n p_n + c_n^u r_n^u + c_n^d r_n^d \\ & + \mathbb{E} [c_n^+ r_n^+(\omega) - c_n^- r_n^-(\omega)] \end{aligned} \quad (3a)$$

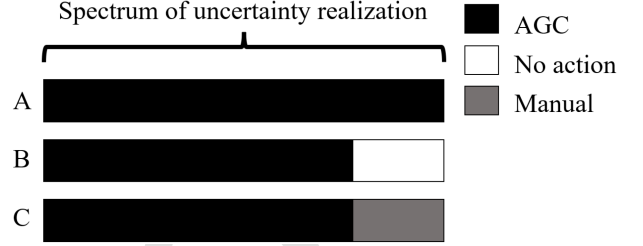


Fig. 2. Actions planned over the spectrum of uncertainty realizations to mitigate imbalances and ensure the reliability of the power system. (a) Model (1) with  $\epsilon = 0$ . (b) Model (1) with  $\epsilon > 0$ . (c) Proposal.

$$\text{s.t.} \quad (1b) - (1f), (2a) - (2e), (1i). \quad (3b)$$

407 Coming back to our example, results from (3) are also included  
 408 in the last row of Table I. Observe that the system operating cost  
 409 is significantly reduced with respect to that of formulation (1)  
 410 with  $\epsilon = 0$ . Furthermore, as in the case of formulation (1)  
 411 with  $\epsilon = 1/3$ , our proposal also renders a solution for which,  
 412 if scenario 3 occurs, the implementation of AGC violates the  
 413 maximum output limit of generator  $g_2$  and the capacity of  
 414 line  $l_1$ . However, unlike the solution to (1), the one delivered  
 415 by our proposal procures 20 MW of upward reserve capacity  
 416 from generator  $g_1$  so that the system operator can release this  
 417 generator from AGC and manually dispatch it at 20 MW under  
 418 scenario 3. For illustrative purposes, Fig. 2 summarizes how the  
 419 mentioned approaches respond to an uncertain scenario.

420 In the following section, we discuss how we solve formula-  
 421 tions (1) and (3).

### III. SOLUTION METHODOLOGY

422 Chance-constrained programs, such as (1) and (3), belong  
 423 to the class of NP-hard problems. In general, there is no finite  
 424 tractable reformulation of the chance-constraint (1h) or (2e).  
 425 As a result, a wide variety of different approaches have been  
 426 proposed to approximate the feasible region determined by these  
 427 constraints, namely, distributionally robust optimization [21];  
 428 the scenario approach [22]; sample average approximation  
 429 (SAA) [23]; and the inner convex approximations based on the  
 430 conditional value-at-risk [24] or ALSO-X [25]. In this work,  
 431 we resort to SAA boosted with bounding, tightening and valid  
 432 inequalities. Consequently, the chance-constrained programs (1)  
 433 and (3) are reformulated as mixed-integer programs (MIP). To  
 434 do that, we assume that  $\omega$  has a finite discrete support defined  
 435 by a collection of atoms  $\{\omega_s \in \mathbb{R}^{|\mathcal{M}|}, s \in \mathcal{S}\}$  and respective  
 436 probability masses  $\mathbb{P}(\omega = \omega_s) = \frac{1}{|\mathcal{S}|} \quad \forall s \in \mathcal{S} = \{1, \dots, |\mathcal{S}|\}$ .  
 437 Accordingly,  $\omega_{ns}$  and  $\Omega_s$  are realizations of the respective ran-  
 438 dom variables under scenario  $s$ , and the decisions  $\alpha_{ns}$ ,  $r_{ns}^+$ , and  
 439  $r_{ns}^-$  for the dispatchable unit at node  $n$  may vary for each scenario  
 440

441  $s$ . We define  $q = \lfloor \epsilon |\mathcal{S}| \rfloor$  and the vector  $\mathbf{y}$  of binary variables  $y_s$   
 442  $\forall s \in \mathcal{S}$ . Thus, the MIP reformulation of problem (3) is written  
 443 as follows:

$$\min_{\Theta} \sum_n c_n p_n + c_n^u r_n^u + c_n^d r_n^d + \frac{1}{|\mathcal{S}|} \sum_s c_n^+ r_{ns}^+ - c_n^- r_{ns}^- \quad (4a)$$

$$\text{s.t. (1b)–(1f)} \quad (4b)$$

$$\sum_n \alpha_{ns} = 0 \quad \forall s \quad (4c)$$

$$r_{ns}^+ - r_{ns}^- = -\Omega_s \beta_n + \alpha_{ns} \quad \forall n, s \quad (4d)$$

$$-r_n^d \leq -\Omega_s \beta_n + \alpha_{ns} \leq r_n^u \quad \forall n, s \quad (4e)$$

$$-\bar{f}_l \leq \sum_n B_{ln} (p_n - \Omega_s \beta_n + \alpha_{ns} + \hat{w}_n + \omega_{ns} - d_n) \leq \bar{f}_l \quad \forall l, s \quad (4f)$$

$$-y_s \bar{r}_n^d \leq \alpha_{ns} \leq y_s \bar{r}_n^u \quad \forall n, s \quad (4g)$$

$$\beta_n, r_{ns}^+, r_{ns}^- \geq 0 \quad \forall n, s \quad (4h)$$

$$\sum_{s \in \mathcal{S}} y_s \leq q \quad (4i)$$

$$y_s \in \{0, 1\} \quad \forall s \quad (4j)$$

444 where the set of decision variables is  $\Theta = (p_n, r_{ns}^-, r_{ns}^+,$   
 445  $r_g^d, r_g^u, y_s, \alpha_{ns}, \beta_n)$ . Constraints (4g)–(4j) represent the sample-  
 446 based MIP reformulation of the joint chance-constraint (2e).  
 447 For a given scenario  $s \in \mathcal{S}$ , the inequalities (4g) establish that a  
 448 manual adjustment to the production of the dispatchable unit at  
 449 node  $n$  in scenario  $s$  can only be done when  $y_s = 1$ . Otherwise,  
 450 if  $y_s = 0$ , the power forecast error must be handled by the  
 451 AGC. Expression (4i) ensures that the probability of the joint  
 452 chance-constraint is met and (4j) enforces the binary character  
 453 of variables  $y_s$ . A MIP reformulation for the SAA of (1) can be  
 454 found in [26].

455 As mentioned above, problem (4) [and the SAA-based reform-  
 456 ulation of (1) too] becomes rapidly intractable as the power  
 457 system size and/or the number of scenarios  $|\mathcal{S}|$  grows. To al-  
 458 leviate this issue, we make use of the methodology proposed  
 459 in [26], where a synergistic combination of constraint screen-  
 460 ing and valid inequalities is exploited. In particular, line flow  
 461 constraints that remain nonbinding for all scenarios  $s \in \mathcal{S}$  have  
 462 been screened out. The identification of these constraints is  
 463 carried out by computing the worst-case flow per line  $l$  and  
 464 per scenario  $s$  in both directions over a relaxation of problem  
 465 (4). Essentially, this involves solving  $2 \times |\mathcal{S}|$  linear programs  
 466 per line  $l$  maximizing (minimizing) the corresponding line flow.  
 467 If the respective maximum (minimum) line flow in scenario  
 468  $s$  is strictly smaller (greater) than (minus) the line capacity  
 469  $\bar{f}_l$  ( $-\bar{f}_l$ ), the  $\leq$ -constraint ( $\geq$ ) in (4f) can be safely removed  
 470 from (4). Furthermore, to tighten the relaxed LP formulation  
 471 of (4), we introduce the valid inequalities developed in [26],  
 472 which guarantee that, in at least  $(1 - \epsilon)$ -percentage of scenarios,

---

**Algorithm 1:** Adaptation of ALSO-X.
 

---

Input: Stopping tolerance parameter  $\delta$

**Require:** Relax the integrality of  $\mathbf{y}$

- 1:  $\underline{q} \leftarrow 0, \bar{q} \leftarrow \lfloor \epsilon |\mathcal{S}| \rfloor$
- 2: **while**  $\bar{q} - \underline{q} \geq \delta$  **do**
- 3: Set  $q = (\underline{q} + \bar{q})/2$  and retrieve  $\Theta^*$  as an optimal solution to (4).
- 4: Set  $\underline{q} = q$  if  $\mathbb{P}(\mathbf{y}^* = 0) \geq 1 - \epsilon$ ; otherwise,  $\bar{q} = q$
- 5: **end while**

Output: A feasible solution of model (4).

---

constraints (4e) and (4f) must be individually satisfied by the 473  
 deployment of AGC only. 474

Alternatively, we have also implemented an adaptation of the 475  
 inner convex approximation ALSO-X [25], which is able to 476  
 identify good feasible solutions of problem (4). As the original 477  
 approximation algorithm, our adaptation works iteratively. It 478  
 first relaxes the integrality of  $\mathbf{y}$  and then enters a loop whose 479  
 core step is to perform a bisection search over parameter  $q$ . 480  
 A pseudocode is provided in Algorithm 1. 481

#### IV. EVALUATION PROCEDURE 482

In this section, we outline the procedure for evaluating the 483  
 performance of the two approaches compared in this article, 484  
 namely, as follows. 485

- 1) The joint chance-constrained problem with AGC only 486  
 formulated in (1) and denoted as AGC- $\epsilon$  hereinafter. For 487  
 $\epsilon = 0$ , the constraints must be satisfied for all scenarios 488  
 and model (1) is formulated as a linear program. For  $\epsilon \neq 0$ , 489  
 model (1) is reformulated as a MIP problem and efficiently 490  
 solved using the procedure described in [26]. 491
- 2) The joint chance-constrained problem with both auto- 492  
 matic and manual generation control formulated in (3) 493  
 and denoted as AMGC- $\epsilon$ . Notice that for  $\epsilon = 0$ , the results 494  
 obtained by AGC-0 and AMGC-0 are the same. For  $\epsilon \neq 0$ , 495  
 model (3) is reformulated as the MIP model (4) and solved 496  
 using the procedure described in Section III. The approach 497  
 that solves model (4) using the heuristic procedure de- 498  
 scribed in Algorithm 1 is denoted as AMGC-H- $\epsilon$ . 499

First, let  $(p_n^*, r_g^{d,*}, r_g^{u,*}, \beta_n^*)$  denote the optimal dispatch and 500  
 reserve capacity decisions delivered by AGC- $\epsilon$ , AMGC- $\epsilon$ , or 501  
 AMGC-H- $\epsilon$  with the in-sample scenario set  $\mathcal{S}$ . We evaluate the 502  
 performance of these decisions on an out-of-sample scenario 503  
 set denoted by  $\mathcal{S}'$  and indexed by  $s'$ , with  $|\mathcal{S}| \ll |\mathcal{S}'|$ . Each out- 504  
 of-sample scenario  $s'$  is characterized by the realization of the 505  
 forecast errors  $\omega_{ns'}$  and the system wise aggregate forecast error 506  
 $\Omega_{s'}$ , with  $\Omega_{s'} = \sum_{n \in \mathcal{N}} \omega_{ns'}$ . For each scenario  $s'$ , we formulate 507  
 the following real-time operation problem: 508

$$\min_{\Psi} \sum_n c_n p_n^* + c_n^u r_n^{u,*} + c_n^d r_n^{d,*} + c_n^+ r_{ns'}^+ - c_n^- r_{ns'}^- + P(\Delta_{ns'}^+ + \Delta_{ns'}^-) \quad (5a)$$

$$\text{s.t. } \sum_n \alpha_{ns'} + \Delta_{ns'}^+ - \Delta_{ns'}^- = 0 \quad (5b)$$



$$r_{ns'}^+ - r_{ns'}^- = -\Omega_{s'}\beta_n^* + \alpha_{ns'} \quad \forall n \quad (5c)$$

$$-r_n^{d,*} \leq -\Omega_{s'}\beta_n^* + \alpha_{ns'} \leq r_n^{u,*} \quad \forall n \quad (5d)$$

$$-\bar{f}_l \leq \sum_n B_{ln}(p_n^* - \Omega_{s'}\beta_n^* + \alpha_{ns'} + \hat{w}_n + \omega_{ns'} - d_n + \Delta_{ns'}^+ - \Delta_{ns'}^-) \leq \bar{f}_l \quad \forall l \quad (5e)$$

$$r_{ns'}^+, r_{ns'}^-, \Delta_{ns'}^+, \Delta_{ns'}^- \geq 0 \quad \forall n. \quad (5f)$$

509 Note that  $\Psi = (r_{ns'}^+, r_{ns'}^-, \alpha_{ns'}, \Delta_{ns'}^+, \Delta_{ns'}^-)$  where  $\Delta_{ns'}^+$  and  
 510  $\Delta_{ns'}^-$  are two slack variables that quantify the positive and  
 511 negative power deviations at each node  $n$ , respectively. These  
 512 deviations are penalized in the objective function through param-  
 513 eter  $P$ , which is to be set large enough so that scenario  
 514  $s'$  is counted as *infeasible* if any of the corresponding slack  
 515 variables takes on a strictly positive value. For each scenario  
 516  $s'$ , model (5) determines the reserve deployments to keep the  
 517 network balanced at the minimum cost. Note that constraints  
 518 (5b)–(5f) are equivalent to constraints (4c)–(4h) but with the  
 519 addition of the slack variables  $\Delta_{ns'}^+$  and  $\Delta_{ns'}^-$ , which guarantee  
 520 the feasibility of model (5) for any scenario realization.

521 Using the solution to model (5), we split the out-of-sample  
 522 scenario set  $\mathcal{S}'$  into three subsets as follows. First, we solve  
 523 model (5) with variables  $\alpha_{ns'}$ ,  $\Delta_{ns'}^+$ , and  $\Delta_{ns'}^-$  fixed to 0, that is,  
 524 enforcing that forecast errors can only be handled by AGC. If  
 525 the problem is feasible, the scenario  $s'$  belongs to subset  $\mathcal{S}'_A$  and  
 526 the real-time operation cost is denoted by  $C_{s'}$ . If this problem  
 527 is infeasible, we solve model (5) without fixing any variable.  
 528 If  $\max(\Delta_{ns'}^+, \Delta_{ns'}^-) = 0$ , then the forecast errors can be offset  
 529 using automatic and manual reserves, and scenario  $s'$  is included  
 530 in subset  $\mathcal{S}'_M$ . Finally, if  $\max(\Delta_{ns'}^+, \Delta_{ns'}^-) > 0$ , then automatic  
 531 and manual reserves are not enough to maintain the power bal-  
 532 ance and power deviations occur during the real-time operation.  
 533 In that case, scenario  $s'$  belongs to the subset  $\mathcal{S}'_D$ . In the next  
 534 section, we evaluate the performance of the different approaches  
 535 by comparing the percentage of scenarios that belong to each  
 536 subset, as well as the expected cost of the real-time operation.

## 537 V. NUMERICAL RESULTS

538 In this section, we compare the performance of the different  
 539 approaches presented in Section II using modified versions of the  
 540 IEEE-118 and IEEE-300 test systems widely employed in the  
 541 technical literature on the topic. The 118-bus system (medium  
 542 case) shows the performance of our novel model in a worst-case  
 543 scenario where very few generators can deploy reserve and either  
 544 have a very cheap or very expensive marginal cost. On the other  
 545 hand, the 300-bus system (large case) illustrates its performance  
 546 in a larger system where, in addition, more flexibility is available  
 547 by the presence of more generators with the ability to back up.

### 548 A. Medium Case: IEEE-118

549 The IEEE-118 test system has 118 nodes, 19 generators, and  
 550 186 transmission lines, and the original data pertaining to this  
 551 system are publicly available in the repository [27]. We assume  
 552 that six generators can provide reserves, and their corresponding  
 553 data are given in Table II. Notice that units 12, 65, and 111  
 554 have a much higher production cost than units 49, 61, and 100.

TABLE II  
GENERATORS WITH CAPABILITY TO PROVIDE RESERVE

$n$	$c_n$	$c_n^-$	$c_n^+$	$c_n^d/c_n^u$	$\bar{r}_n^d/\bar{r}_n^u$
12	124.6	99.7	149.5	24.9	85
49	16.7	13.3	20.0	3.3	223
61	16.1	12.8	19.3	3.2	195
65	100.0	80.0	120.0	20.0	441
100	12.6	10.1	15.1	2.5	653
111	110.0	88.0	132.0	22.0	79

TABLE III  
MEDIUM CASE: OUT-OF-SAMPLE PERFORMANCE COMPARISON

	$ \mathcal{S}'_A $	$ \mathcal{S}'_M $	$ \mathcal{S}'_D $	$\mathbb{E}[C_{s'}]$ (k€)
AGC-0	99.56%	0.16%	0.28%	73.65
AGC-5	94.12%	0.17%	5.71%	53.04
AMGC-5	94.30%	5.41%	0.29%	60.15
AMGC-H-5	94.77%	4.98%	0.25%	61.05

555 For these six units, the reserve deployment costs are computed  
 556 as  $c_n^- = 0.8c_n$  and  $c_n^+ = 1.2c_n$ , and the reserve capacity costs  
 557 are  $c_n^d = c_n^u = 0.2c_n$ . Besides, we add 25 wind power plants  
 558 throughout the system as suggested in [28]. We consider that  
 559 the wind power forecast error is normally distributed, i.e.,  $\omega \sim$   
 560  $N(\mathbf{0}, \Sigma)$ , where  $\mathbf{0}$  and  $\Sigma$  represent, respectively, the zero vector  
 561 and the covariance matrix. We also assume that the standard  
 562 deviation of  $\omega_n$  at node  $n$  is a 15% of the wind power forecast  
 563  $w_n$ . The uncertainty pertaining to the renewable generation of  
 564 the wind farms is characterized using 1000 scenarios, that is,  
 565  $|\mathcal{S}| = 1000$ . Finally, the penalty cost  $P$  due to deviations is twice  
 566 the production cost of the most expensive generator. All data of  
 567 this modified 118-bus system are available at [29].

568 To provide meaningful statistics, each method is run for ten  
 569 different sets of randomly generated scenarios. Accordingly, we  
 570 report results averaged over these ten instances. All optimization  
 571 problems have been solved using GUROBI 9.1.2 [30] on a  
 572 Linux-based server with CPUs clocking at 2.6 GHz, 6 threads,  
 573 and 16 GB of RAM. In all cases, the optimality GAP has been  
 574 set to  $10^{-9}\%$  and the time limit to 10 h.

575 We compare the different approaches following the out-  
 576 of-sample evaluation procedure described in Section IV with  
 577 100 000 different scenarios drawn from the same distribution,  
 578 that is,  $|\mathcal{S}'| = 100\,000$ . We compare the results of four dif-  
 579 ferent approaches, namely: 1) AGC-0, which corresponds to  
 580 the joint chance-constrained OPF model (1) with  $\epsilon = 0\%$  (i.e.,  
 581 all scenarios must be satisfied); 2) AGC-5, which is the joint  
 582 chance-constrained OPF model (1) with  $\epsilon = 5\%$  (that is, 50 sce-  
 583 narios may have violated constraints); 3) the proposed AMGC-5  
 584 approach, which is the proposed stochastic OPF model (3) with  
 585  $\epsilon = 5\%$  (50 scenarios may use manual adjustments to redispatch  
 586 generators); and 4) AMGC-H-5, which is the proposed stochas-  
 587 tic OPF model (3) solved with the heuristic ALSO-X procedure  
 588 to solve AMGC-5. The results given in Table III include the  
 589 following.

- 590 1) The percentage of scenarios, in which the forecast errors  
 591 are handled using AGC only  $|\mathcal{S}'_A|$ .
- 592 2) The percentage of scenarios, in which manual redispatch  
 593 is required to keep power balance throughout the network  
 594  $|\mathcal{S}'_M|$ .



TABLE IV  
COMPARISON OF DECISIONS MADE BY AGC AND AMGC

	Cheap Generators			Expensive Generators		
	$\beta$	$r^d$	$r^u$	$\beta$	$r^d$	$r^u$
AGC-0	0.77	533.6	538.5	0.23	160.1	162.5
AGC-5	1.00	509.4	364.5	0.00	0.0	0.0
AMGC-5	0.99	684.7	386.3	0.01	7.9	314.7
AMGC-H-5	0.96	675.7	395.3	0.04	16.9	305.6

595 3) The percentage of scenarios, in which automatic and manual reserves are not enough to offset power imbalances and therefore, power deviations are inevitable and the system security is compromised  $|\mathcal{S}'_D|$ .

599 4) The total expected cost.

600 As expected, AGC-0 gives very conservative and expensive solutions, but is able to handle power imbalances using only AGC in 99.56% of the scenarios and only has 0.28% scenarios, in which system security is compromised. In comparison, we observe that the expected cost of the AGC-5 solutions is 28% lower on average than those of AGC-0 and that AGC activation is sufficient to guarantee system security in 94.12% of scenarios (close to the desired violation probability of 95%). However, the AGC-5 are not able to offset power imbalances with both types of reserves in 5.71% of the scenarios, thus compromising the safety of the system. The proposed AMGC-5 approach is able to compute dispatch solutions while taking into account both automatic and manual reserves. As expected, imbalances are compensated with AGC in 94.30% of the scenarios, and manual reserves are only required in 5.41% of them. Note that these percentages are very close to the desired values of 95% and 5%. Although there is still 0.29% scenarios in which system security is compromised, the proposed methodology reduces the expected cost by 18% with respect to AGC-0 (which has reliability levels). Finally, the results obtained with the heuristic ALSO-X algorithm AMGC-H-5 are slightly more conservative and expensive than those of AMGC-5. However, these results confirm that Algorithm 1 provides a good feasible solution to formulation (4).

624 To give more details on the out-of-sample performance of the different approaches, Table IV gathers a summary of the OPF decisions  $\beta_n^*$ ,  $r_n^{d,*}$ , and  $r_n^{u,*}$ . For conciseness, we aggregate the units providing reserves into cheap and expensive generators. Interestingly, AGC-0 yields more conservative OPF decisions since both cheap and expensive generators are dispatched to provide AGC. Conversely, the other methods mainly allocate AGC to cheap generators only. Notice that in the case of AGC-5, the values of  $\beta$ ,  $r^d$ , and  $r^u$  are 0 for expensive generators, which means that these units will not be available for manual reserve during the real-time operation of the power system and therefore, the probability of incurring in dangerous power deviations increases. Conversely, both AMGC-5 and AMGC-H-5 procure more reserve capacities so that cheap and expensive generators can be effectively and efficiently redispatched to minimize the real-time operation cost while reducing power deviations.

640 To further illustrate the differences between the methods compared in this section, we compute for each out-of-sample scenario  $s'$  the overall level of infeasibility, quantified by the

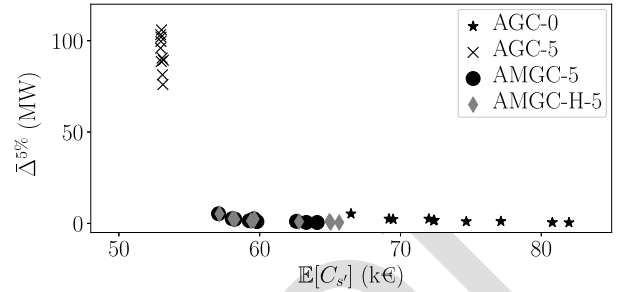


Fig. 3. Expected cost versus the average deviation of the 5% scenarios with the largest deviations for each of the four considered methods. The results for AGC-0 (denoted by stars) are clustered to the lower right of the figure, indicating that the method finds very reliable, but also very costly solutions. The results for AGC-5 (denoted by crosses) are clustered to the upper left of the figure, indicating that this method finds less costly, but also much less reliable solutions. The results for the proposed approach AMGC-5 and the associated heuristic method AMGC-H-5 are clustered in the middle of the figure, indicating that the proposed method finds a good tradeoff between cost and reliability. Note that the markers for AMGC-5 and AMGC-H-5 partially overlap, indicating that the heuristic AMGC-H-5 method identifies close-to-optimal solutions.

total deviation  $\Delta_{s'}$  as follows: 643

$$\Delta_{s'} = \sum_n (\Delta_{n,s'}^+ + \Delta_{n,s'}^-).$$

Fig. 3 plots the average value of  $\Delta_{s'}$  for the 5% scenarios with largest deviations ( $\bar{\Delta}_{s'}^{5\%}$ ) versus the expected cost for each method and each of the ten independent samples. As observed, AGC-0 involves very low deviation levels but the highest expected cost. Under AGC-5, the expected cost is decreased at the expense of increasing the system deviations. Finally, the proposed methods AMGC-5 and AMGC-H-5 manage to maintain similarly low levels of deviations as AGC-0, but at a significantly lower cost. 652

To conclude this case study, we provide the average computational times of the different approaches. Since AGC-0 is formulated as a linear programming problem, it takes 6.1 s on average to be solved. Using the efficient solution procedure proposed in [26], AGC-5 is solved in 14.3 s. Since the proposed AMGC-5 requires the use of extra variables to properly model the deployment of manual reserves, its average computational time increases up to 3288.5 s. Nevertheless, the heuristic procedure described in Section III is able to reduce this time to 73.6 s with a very slight impact on the performance of AMGC-5. 662

## B. Large Case: IEEE-300 663

The IEEE-300 test system has 300 nodes, 57 generators, and 411 transmission lines, and the original data pertaining to this system are also publicly available in the repository [27]. This system has 15 generators with the ability to use reserve, i.e., it is possible to size the reserve. Small wind farms have been distributed throughout the system, a total of 119, with a share of 40%. The forecast error is also normally distributed, as in the IEEE-118 case study, and has a standard deviation of 15% of the predicted value (the optimization setup of the solver, and the number of in-sample and out-of-sample scenarios is the same 673

TABLE V  
LARGE CASE: OUT-OF-SAMPLE PERFORMANCE COMPARISON

	$ S'_A $	$ S'_M $	$ S'_D $	$\mathbb{E}[C'_{sr}]$ (k€)
<b>AGC-0</b>	99.22%	0.21%	0.56%	242.73
<b>AGC-5</b>	93.86%	0.39%	5.75%	238.51
<b>AMGC-5</b>	94.31%	5.03%	0.54%	239.64
<b>AMGC-H-5</b>	94.78%	4.68%	0.65%	240.92

too). All data of this modified 300-bus system are available at [29].

As can be seen in Table V, in this system, results similar to those in Table III are obtained. AGC-0 obtains the most conservative and expensive solution, where 99.22% of the scenarios are handled by AGC. On the contrary, AGC-5 obtains a solution that is approximately 1.8% cheaper<sup>1</sup> than AGC-0, but is much less reliable as the system's security is not guaranteed in 5.75% of the scenarios. For the proposed approach AMGC-5, imbalances are compensated with AGC in 94.31% of the scenarios and manual adjustments are required in 5.03% of them. Its reliability is similar to AGC-0, with only about 0.5% of samples with system insecurity. However, the AMGC-5 solution is 1.3% cheaper. This again highlights the ability of the proposed model to provide more reliable and cheaper solutions compared with existing methods.

As mentioned above, an unfortunate aspect of the proposed AMGC-5 model is that it requires significantly higher computational time compared with AGC-0 and AGC-5. Both AGC-0 and AGC-5 can be solved in approximately 20 and 100 s, respectively. In contrast, AMGC-5 exceeds the allocated time limit of 10 h, and terminates with a final MIPGap achieved in the range of 0.2%–0.5%. One option to reduce computation time is to leverage the proposed heuristic method AMGC-H-5 instead of AMGC-5. For the 300-bus system, AMGC-H-5 solves in about 170 s. This increase in computation time comes at the expense of slightly more expensive solutions. While AMGC-H-5 is as reliable or more reliable than AMGC-5 and AGC-5, it does have 0.5% higher operating costs than AMGC-5. Given that this cost is still significantly lower than that of AGC-0 and the reliability of the solution is much better than for AGC-5, we conclude that the heuristic method AMGC-H-5 is a good option for scaling our proposed optimization model to larger systems.

## VI. CONCLUSION

Existing approaches to solve the stochastic OPF are either overly conservative and expensive, or leave the system vulnerable to low-probability, high-impact events. To address this issue, we present a novel stochastic optimal power flow formulation that distinguishes between “normal” operation conditions in which power deviations are balanced with AGC only, and “adverse” operation under which manual redispatch actions are required. As a result, our approach yields solutions that are more reliable and less conservative than existing approaches in the literature.

<sup>1</sup>Note that, in this system, the cost difference is much lower because the number of generators with the ability to provide reserve is greater, i.e., it accounts for more flexibility resulting in more optimal affine control policies for AGC-0.

Our model is formulated as a joint chance-constraint program that limits the probability that operators manually adjust the power output of the generators. To assess the contributions of our proposal, we compare it with existing approaches using an illustrative three-bus network and more realistic ones, such as the 118-bus and 300-bus systems. The obtained results for the larger systems demonstrate that the proposed methodology is able to achieve dispatch decisions that maintain almost identical security levels, but are cheaper than approaches that pursue feasibility with AGC actions only under any uncertainty realization. A drawback of our proposed approach is that the computational burden increases due to the modeling of the manual redispatch actions. However, we also suggest an heuristic algorithm to solve the proposed model and verify that the computational time is drastically shortened without causing a significant decline in performance.

While the proposed approach represents a step toward more realistic modeling of reserve activation in stochastic OPF problems, several open questions remain. Avenues for future work include, for example, how to incorporate restrictions on manual reserve activation (such as, e.g., limiting the number of generators that participate in the manual activation), a more detailed and realistic modeling of reserve cost that acknowledges the possible cost difference between automatic AGC reserves and manually activated reserves, as well as a strategy to handle situations in which the problem becomes infeasible (due to, e.g., high levels of uncertainty, severe system congestion, or limited generation capacity).

## ACKNOWLEDGMENT

The authors would like to thank the Supercomputing and Bioinformatics (SCBI) center of the University of Malaga for the computer resources, technical expertise, and assistance.

## REFERENCES

- [1] X. Liu, S. Küçkyavuz, and J. Luedtke, “Decomposition algorithms for two-stage chance-constrained programs,” *Math. Program.*, vol. 157, no. 1, pp. 219–243, 2016.
- [2] M. Shahidepour, H. Yamin, and Z. Li, *Market Operations in Electric Power Systems: Forecasting, Scheduling, and Risk Management*. New York, NY, USA: Wiley, 2003.
- [3] S. Frank, I. Steponavice, and S. Rebennack, “Optimal power flow: A bibliographic survey I,” *Energy Syst.*, vol. 3, no. 3, pp. 221–258, 2012.
- [4] L. Xie et al., “Wind integration in power systems: Operational challenges and possible solutions,” *Proc. IEEE*, vol. 99, no. 1, pp. 214–232, Jan. 2011.
- [5] L. A. Roald, D. Pozo, A. Papavasiliou, D. K. Molzahn, J. Kazempour, and A. Conejo, “Power systems optimization under uncertainty: A review of methods and applications,” *Electric Power Syst. Res.*, vol. 214, 2023, Art. no. 108725.
- [6] J. M. Morales, A. J. Conejo, and J. Perez-Ruiz, “Economic valuation of reserves in power systems with high penetration of wind power,” *IEEE Trans. Power Syst.*, vol. 24, no. 2, pp. 900–910, May 2009.
- [7] R. A. Jabr, S. Karaki, and J. A. Korbane, “Robust multi-period OPF with storage and renewables,” *IEEE Trans. Power Syst.*, vol. 30, no. 5, pp. 2790–2799, Sep. 2015.
- [8] J. Warrington, P. Goulart, S. Mariétoz, and M. Morari, “Policy-based reserves for power systems,” *IEEE Trans. Power Syst.*, vol. 28, no. 4, pp. 4427–4437, Nov. 2013.
- [9] A. Lorca and X. A. Sun, “The adaptive robust multi-period alternating current optimal power flow problem,” *IEEE Trans. Power Syst.*, vol. 33, no. 2, pp. 1993–2003, Mar. 2018.

- 778 [10] W. Van Ackooij, R. Zorgati, R. Henrion, and A. Möller, "Chance constrained programming and its applications to energy management," in 779 *Stochastic Optimization-Seeing the Optimal for the Uncertain*. Nordstedt, 780 Germany: Books on Demand, pp. 291–320, 2011.
- 782 [11] M. Vrakopoulou, K. Margellos, J. Lygeros, and G. Andersson, "Probabilistic 783 guarantees for the N-1 security of systems with wind power generation," 784 in *Reliability and Risk Evaluation of Wind Integrated Power Systems*. 785 Berlin, Germany: Springer, 2013, pp. 59–73.
- 786 [12] D. Bienstock, M. Chertkov, and S. Harnett, "Chance-constrained optimal 787 power flow: Risk-aware network control under uncertainty," *SIAM Rev.*, 788 vol. 56, no. 3, pp. 461–495, 2014.
- 789 [13] M. Lubin, Y. Dvorkin, and S. Backhaus, "A robust approach to chance 790 constrained optimal power flow with renewable generation," *IEEE Trans.* 791 *Power Syst.*, vol. 31, no. 5, pp. 3840–3849, Sep. 2016.
- 792 [14] A. M. Hou and L. A. Roald, "Chance constraint tuning for optimal power 793 flow," in *Proc. Int. Conf. Probabilistic Methods Appl. Power Syst.*, 2020, 794 pp. 1–6.
- 795 [15] A. Esteban-Pérez and J. M. Morales, "Distributionally robust optimal 796 power flow with contextual information," *Eur. J. Oper. Res.*, vol. 306, 797 no. 3, pp. 1047–1058, 2023.
- 798 [16] J. Warrington, P. J. Goulart, S. Mariéthoz, and M. Morari, "Robust reserve 799 operation in power systems using affine policies," in *Proc. IEEE 51st IEEE* 800 *Conf. Decis. Control*, 2012, pp. 1111–1117.
- 801 [17] North American Reliability Corporation (NERC), "Standard BAL-005 - 802 automatic generation control," 2009. [Online]. Available: <https://www.nerc.com/pa/Stand/Pages/Default.aspx> 803
- 804 [18] R. Kannan, J. R. Luedtke, and L. A. Roald, "Stochastic DC optimal power 805 flow with reserve saturation," *Electric Power Syst. Res.*, vol. 189, 2020, 806 Art. no. 106566.
- 807 [19] L. Roald, S. Misra, M. Chertkov, and G. Andersson, "Optimal power 808 flow with weighted chance constraints and general policies for generation 809 control," in *Proc. 54th IEEE Conf. Decis. Control*, 2015, pp. 6927–6933.
- 810 [20] K. Margellos, V. Rostampour, M. Vrakopoulou, M. Prandini, G. Andersson, 811 and J. Lygeros, "Stochastic unit commitment and reserve scheduling: 812 A tractable formulation with probabilistic certificates," in *Proc. Eur. Control* 813 *Conf.*, 2013, pp. 2513–2518.
- 814 [21] G. A. Hanasusanto, V. Roitch, D. Kuhn, and W. Wiesemann, "Ambiguous 815 joint chance constraints under mean and dispersion information," *Operations* 816 *Res.*, vol. 65, no. 3, pp. 751–767, 2017.
- 817 [22] A. Nemirovski and A. Shapiro, "Scenario approximations of chance 818 constraints," in *Probabilistic and Randomized Methods for Design Under* 819 *Uncertainty*. Berlin, Germany: Springer, 2006, pp. 3–47.
- 820 [23] J. Luedtke and S. Ahmed, "A sample approximation approach for opti- 821 mization with probabilistic constraints," *SIAM J. Optim.*, vol. 19, no. 2, 822 pp. 674–699, 2008.
- 823 [24] A. Nemirovski and A. Shapiro, "Convex approximations of chance constrained 824 programs," *SIAM J. Optim.*, vol. 17, no. 4, pp. 969–996, 2007.
- 825 [25] N. Jiang and W. Xie, "ALSO-X and ALSO-X: Better convex approximations 826 for chance constrained programs," *Operations Res.*, 2022.
- 827 [26] Á. Porras, C. Domínguez, J. M. Morales, and S. Pineda, "Tight and compact 828 sample average approximation for joint chance constrained optimal 829 power flow," 2022, *arXiv:2205.03370*.
- 830 [27] Power Grid Lib, "GitHub repository," 2022. [Online]. Available: <https://github.com/power-grid-lib/pglib-opf> 831
- 832 [28] L. Roald, S. Misra, M. Chertkov, S. Backhaus, and G. Andersson, "Chance 833 constrained optimal power flow with curtailment and reserves from wind 834 power plants," 2016, *arXiv:1601.04321*.
- 835 [29] OASYS, "Data of 118-node power system," GitHub repository, 2023. 836 [Online]. Available: [https://github.com/groupoasys/AGC\\_and\\_Manual](https://github.com/groupoasys/AGC_and_Manual_Reserve_CC) 837 *Reserve\_CC*
- 838 [30] Gurobi Optimization, LLC, "Gurobi Optimizer Reference Manual," 2022.



Álvaro Porras received the B.S. degree in industrial technologies engineering, the M.S. degree in industrial engineering, and the Ph.D. degree in power systems from the University of Malaga, Malaga, Spain, in 2018, 2020, and 2023, respectively.

His research interests include energy systems operation and planning, decision-making under uncertainty, and optimization.



Line Roald (Member, IEEE) received the Ph.D. degree in electrical engineering from ETH Zurich, Zurich, Switzerland, in 2016.

She was a Postdoctoral Research Fellow with the Center of Nonlinear Studies, Los Alamos National Laboratory, Santa Fe, NM, USA. She is currently an Associate Professor and Grainger Institute Fellow with the Department of Electrical and Computer Engineering, University of Wisconsin–Madison, Madison, WI, USA. Her research interests include modeling

and optimization of energy systems, with a particular focus on managing uncertainty and risk from extreme weather and renewable energy variability.

Dr. Roald was the recipient of an NSF CAREER award, the Vilas Early-Career Investigator Award, and several best paper awards.



Juan Miguel Morales (Senior Member, IEEE) received the Ingeniero Industrial degree from the University of Málaga, Málaga, Spain, in 2006, and the Ph.D. degree in electrical engineering from the University of Castilla-La Mancha, Ciudad Real, Spain, in 2010.

He is currently a Full Professor with the Department of Mathematical Analysis, Statistics and Operations Research, and Applied Mathematics, University of Málaga. His research interests include fields of data analytics and optimization, decision-making under uncertainty, smart grids, power systems economics, operations and planning, and electricity markets.

877 878 879



Salvador Pineda (Senior Member, IEEE) received the Ingeniero Industrial degree from the University of Málaga, Málaga, Spain, in 2006, and the Ph.D. degree in electrical engineering from the University of Castilla-La Mancha, Ciudad Real, Spain, in 2011.

He is currently an Associate Professor with the Department of Electrical Engineering, University of Málaga. His research interests include power system operation and planning, decision-making under uncertainty, bilevel programming,

machine learning, and statistics.

839 840 841 842 843 844 845 846 847 848

849 850 851 852 853 854 855 856 857 858 859 860 861 862 863 864 865

866 867 868 869 870 871 872 873 874 875 876 877 878 879

Q5

Q3

Q4

880 881 882 883 884 885 886 887 888 889 890 891 892